Journal of
Marine Science and Engineering

MDPI

Article

Application of Buoyancy Support System to Secure Residual Buoyancy of Damaged Ships

Gyeong Joong Lee [1], Jang-Pyo Hong [2], Kwang Keun Lee [3] and Hee Jin Kang [2,*]

1 Advanced Ship Research Division, KRISO, Daejeon 34103, Republic of Korea
2 Alternative Fuels and Power System Research Center, KRISO, Daejeon 34103, Republic of Korea
3 CTO/Leeyoung SND Co., Ltd., Ansan-si 15434, Republic of Korea
* Correspondence: hjkang@kriso.re.kr; Tel.: +82-10-5738-5117

Abstract: SOLAS (Safety of Life at Sea), which was first enacted in 1914 as a result of the Titanic disaster, presents mandatory requirements for ship safety, such as the adoption of watertight bulkheads. However, ship accidents continue to occur despite the development and application of numerous safety technologies. In the case of a marine accident, the risk of sinking or capsizing due to flooding can be reduced by subdividing the watertight area, but shipbuilding costs, the weight increase for light ships, and the intact stability of the vessel must be considered together. For this reason, in this study, a BSS (buoyancy support system) was designed in accordance with ISO 23121-1 and ISO 23121-2. The characteristics of watertight and non-watertight spaces were reviewed and the BSS was implemented for a small car ferry. By applying additional safety technologies while securing economic feasibility in terms of ship construction and operation, an alternative to reduce the loss of human lives, environmental damage, and property losses in the case of a ship accident was proposed.

Keywords: buoyancy support system; flooding; accidents (incidents); evacuation; stability; damaged ships

Citation: Lee, G.J.; Hong, J.-P.; Lee, K.K.; Kang, H.J. Application of Buoyancy Support System to Secure Residual Buoyancy of Damaged Ships. *J. Mar. Sci. Eng.* **2023**, *11*, 656. https://doi.org/10.3390/jmse11030656

Academic Editor: Md Jahir Rizvi

Received: 31 December 2022
Revised: 8 March 2023
Accepted: 14 March 2023
Published: 20 March 2023

1. Introduction

1.1. Previous Studies

Various technical alternatives for delaying or preventing the sinking or capsizing of ships damaged by accidents have been studied and presented. BSS is also one of the alternatives and aims to secure the remaining buoyancy of ships with damage beyond the design standard. A preceding study, entitled, "A concept study for the buoyancy support system based on the fixed fire-fighting system for damaged ships," published in *Ocean Engineering Journal*, Vol. 155(1) [1], presented the results of the research on technical considerations in applying BSS to cargo ships and passenger ships. Figure 1 shows concept of the BSS.

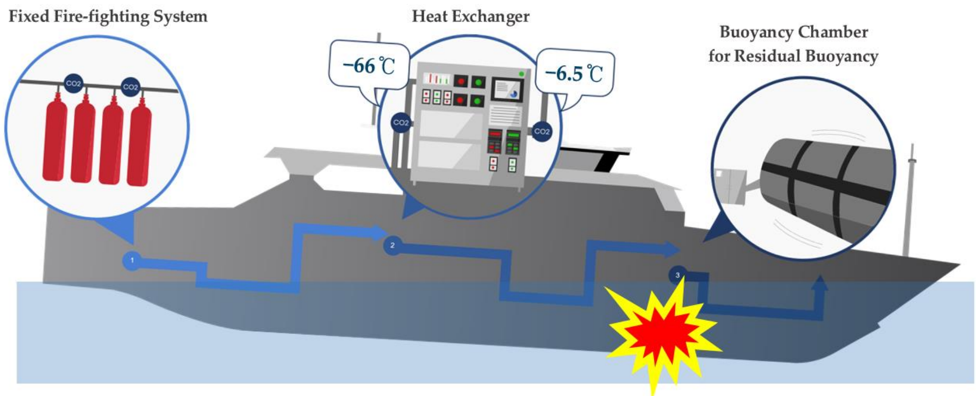

Figure 1. Concept of the BSS [1].

The conceptual design of a BSS obtained AIP (Approval In Principal) from Korea Register of Shipping in 2018. Two ISO standards, “ISO 23121-1, Inflatable Buoyancy Support Systems Against Flooding of Ships—Part 1: Gas Supply System” [2], and “ISO 23121-2, Inflatable Buoyancy Support Systems Against Flooding of Ships—Part 2: Buoyancy Chamber” [3] for the requirements and composition of BSS were published at the end of 2019. In addition to the BSS presented in this study, various alternatives for securing the residual buoyancy of damaged ships have been studied, as shown in Table 1.

Table 1. Research for the improvement of survivability of damaged ships.

Research Topic	Key Findings	References
Buoyancy support system based on fixed fire-fighting system	Proposed a concept for a buoyancy support system based on the fixed fire-fighting system, which could be activated to enhance stability in damaged ships.	Kang et al., 2018 [1]; Kang et al., 2022 [4]
Design for an anti-capsize ship	Design for an anti-capsize ship using self-righting arm force for patrol vessels.	Trimulyono et al., 2023 [5]
Survivability of damaged ships	High-expansion foam can be an effective risk control option to increase passenger ship safety during flooding.	Vassalos et al., 2022 [6]
Active flooding mitigation system	Active flooding mitigation system to enhance stability in a damaged RoPax ship	Valanto et al., 2022 [7]
Refloating a damaged ship with salvage pontoon	Calculation was conducted on refloating a damaged ship with salvage pontoon.	Pan et al. 2020 [8]
Parametric roll avoidance	Proposed a control strategy using rudder movement to suppress parametric roll.	Bačkalov et al., 2016 [9]
Improvement of ship stability and safety in damaged condition	Explored several operational measures to enhance ship stability and safety, including flooding control and the use of bilge pumps.	Boulougouris et al., 2016 [10]
Foam resin-based damage stability recovery system	Proposed the use of foam resin as a damage stability recovery system, which can prevent or delay water ingress and improve ship survivability.	Vassalos et al., 2016 [11]
Inner ship structure buoyancy support system for cargo vessels	Developed the Surfacing System for Ship Recovery (SUSY), which is an inner ship structure designed to prevent cargo vessels from losing stability.	Smith et al., 2011 [12]

The application of new safety technologies, such as BSS, can be realized when the loss of lives, environmental damage, and property losses in the event of an accident can be minimized at an affordable cost for the ship owner. In the previous study, the BSS presented the concept of using a fixed fire main installed on a ship to charge the buoyancy chamber. It was also suggested that the buoyancy chamber may be configured in a three-dimensional shape or comprise multiple cylinders for installation in a complex inner ship space, such as a machinery room. This can reduce the need to install a separate filling material storage tank, transport pipe, and power and data line compared to the concept of using foam. The three-dimensional buoyancy chamber has the advantage of securing a work space and the reusability of the BSS-installed space after an accident. For this reason, in this study, the characteristics of watertight and non-watertight spaces were reviewed for the installation of BSS, and the process of designing, manufacturing, and installing BSS for a small car ferry was carried out in areas with a risk of capsizing or sinking in a flooding accident. In this paper, real cases and plans for ship implementation from the initial concept, which was introduced as a proceeding at PRADS 2022, are studied in more detail [4].

1.2. Design Alternatives

The method of subdividing watertight spaces improves the stability of a ship without installing a separate system that secures residual buoyancy, such as a BSS. However, in this case, the stability effect due to the increase in both the weight of the hull and shipbuilding costs is problematic. Therefore, ships are designed at a level that satisfies SOLAS and classification rules, except for special cases such as naval vessels. The installation of a BSS can primarily be considered for areas near water lines with a statistically high risk of accidents. Among these areas, there are those with complex internal structures, such as machinery rooms, areas that remain watertight during operation, and areas that are non-watertight due to openings such as ducts. Figure 2 briefly shows the flooding characteristics of watertight and non-watertight spaces. Even if a ship is damaged, the watertight space may contain trapped air spaces, which provide residual buoyancy. Therefore, watertight spaces can increase the stability of a ship, while vented spaces cannot.

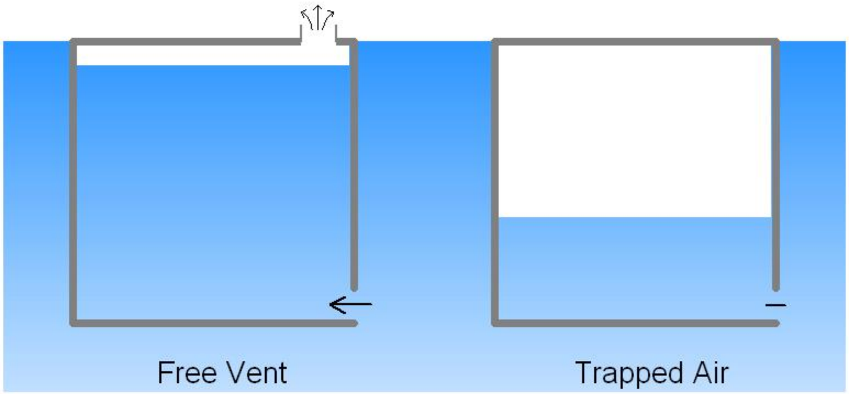

Figure 2. Comparison of flooding characteristics between watertight (trapped air) and non-watertight (free vent) spaces; Arrows show the flow of water (blue colored) and air (white colored) and hyphen means there are no flow of water.

In order to observe the effect of the vent characteristic (watertight or not) on the stability of a ship in case of damage, flooding simulations were carried out for side damage scenarios. For flooding water treatment in the previous study [1], KRISO's in-house simulation tool, SURVSHIP, was employed, which was also used in the former version of SMTP [13,14]. In the simulation, sloshing effects were not considered and the flooded water level in the damaged compartment of the hull was calculated using quasi-static methods.

Table 2 shows the specifications of an example ship used for the comparison of flooding characteristics in watertight and non-watertight spaces. The ship has two internal decks, each with five zones on either side (port and starboard), with a long center corridor. Each zone has a door connecting to the center, with a size of 1 m (width) × 2 m (height). All doors are open, and the center is ventilated with an exhaust area of 2 m^2. The deck height was set at 6 m. The non-watertight example has an air duct system, with the inlet of the duct located at the ceiling of each zone near the center corridor. The duct is fully opened, so the freely vented situation was assumed. The damage was assumed to take place in the portside Zone 2 of the 1st deck.

Figures 3 and 4 show the results of progressive flooding simulations, including sinkage, roll angle, and filling ratios of each zone. In Figure 3, for the watertight model, the filling ratios of compartments in the portside converge to about 0.6 (these compartments are located underwater because of sinking and roll angle), leaving nearly 40% of the space as air-trapped, playing a residual buoyancy role. The watertight model ship stops sinking at 3.2 m of sinkage, even though it heels to 17 degrees port.

Table 2. Specifications of the example ship for flooding characteristic comparison.

Data	Value
LBP	162.10 m
Breadth	27.60 m
Draught	7.00 m
Depth	20.93 m
Displacement	18,060.00 m^3
KG	12.27 m
GM	3.15 m

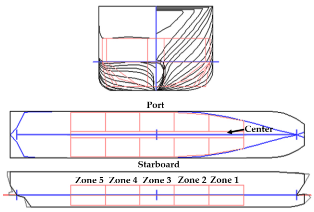

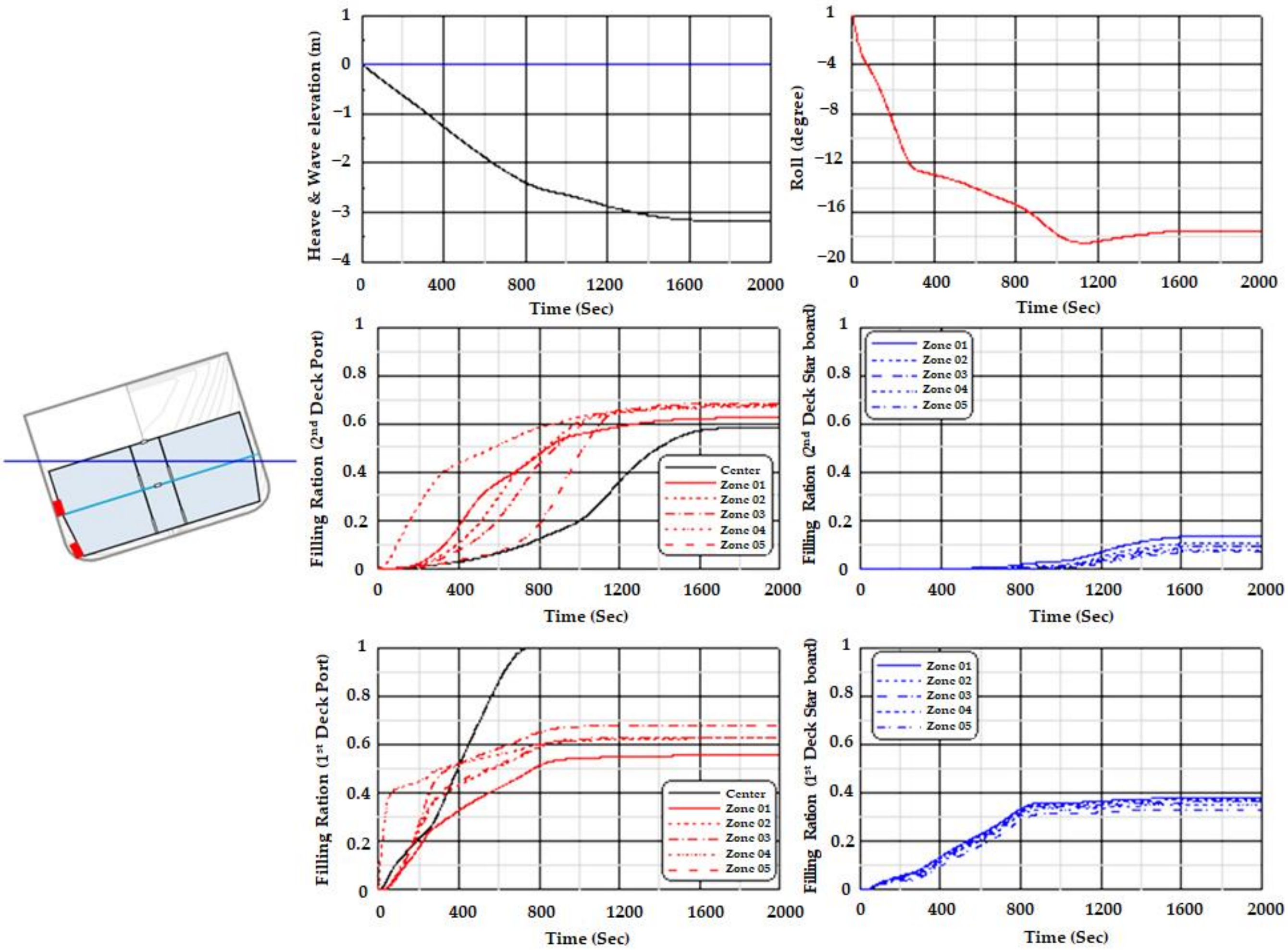

Figure 3. Analysis results of flooding charateristics in the watertight area.

Figure 4 shows the results for a non-watertight model ship. The filling ratios of the compartments in the 1st deck portside reach nearly 1, i.e., fully flooded. The other filling ratios continue to grow, and the ship may sink finally. From the results, it can be said that watertight compartments can increase the stability of a ship, and the locations of the inlets of the vent system should be carefully considered; they may turn a watertight compartment into a non-watertight one if the inlet position height is high up to the ceiling.

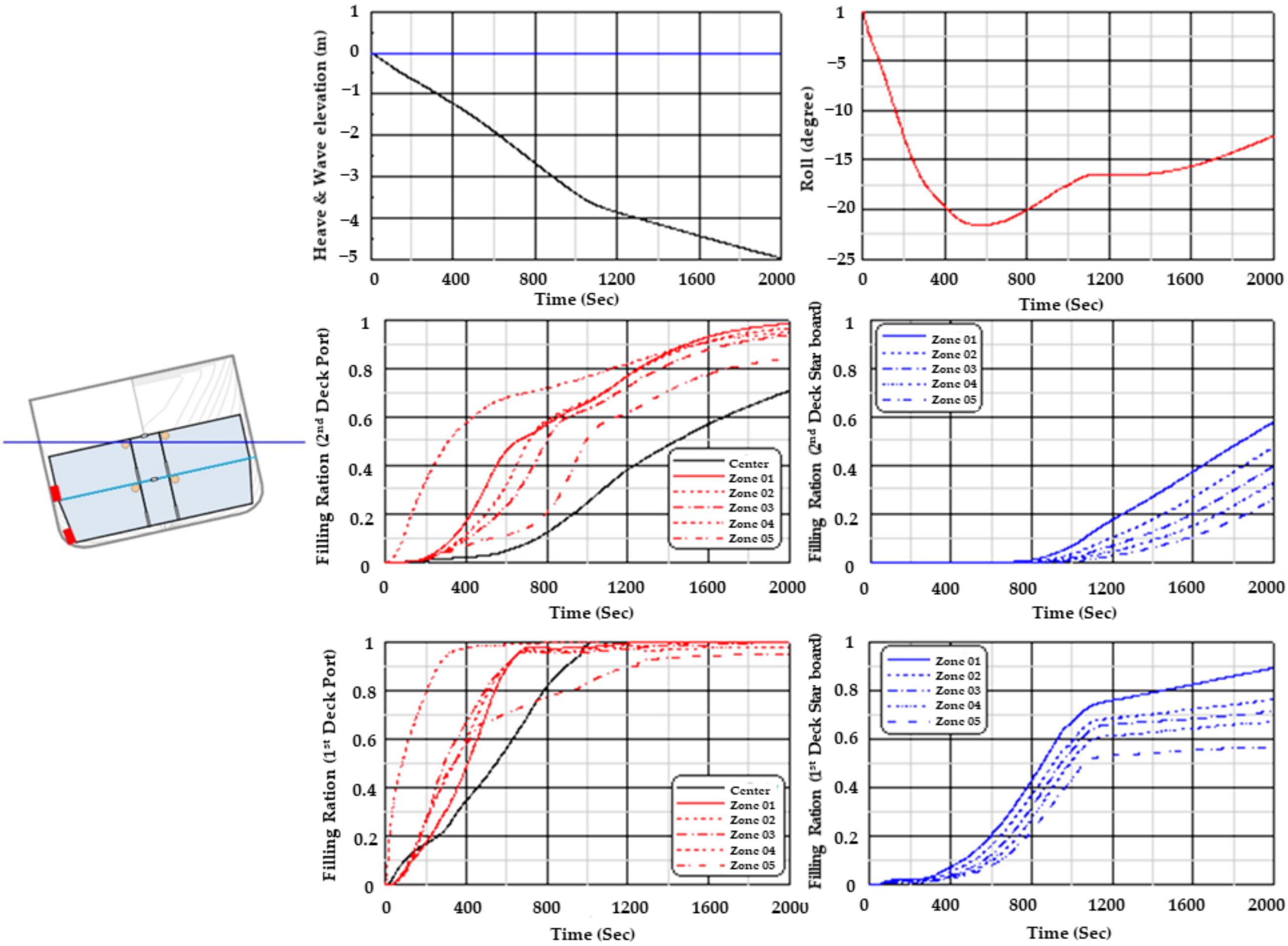

Figure 4. Analysis result of flooding characteristics of non-watertight area.

Besides the sinking instability described above, transverse stability (capsizing stability) due to flooding should also be considered.

If the amount of the flooded volume is ∇_F, the location of the flooded part is y_F and z_F from the center line and base line, respectively, and the length and width of the free surface of the flooded part are l_F and s_F, respectively. The increase in mass and displacement is as follows.

$$\Delta' = \Delta + \rho\nabla_F \tag{1}$$

$$\nabla' = \nabla + \nabla_F \tag{2}$$

When A_{WP} is the ship waterline area, the draught (d) change due to flooding can be drawn as follows.

$$\delta d = \frac{\nabla_F}{A_{WP}} \tag{3}$$

$$d' = d + \frac{\nabla_F}{A_{WP}} \tag{4}$$

The height of the center of buoyancy (KB) can be expressed as follows if the waterline shape is assumed wall-sided.

$$\begin{aligned} KB' &= \frac{KB\times\nabla + \left(d + \frac{1}{2}\frac{\nabla_F}{A_{WP}}\right)\times\nabla_F}{\nabla+\nabla_F} \\ &= KB + \left(\left(d + \frac{1}{2}\frac{\nabla_F}{A_{WP}}\right) - KB\right)\frac{\nabla_F}{\nabla} - \left(d + \frac{1}{2}\frac{\nabla_F}{A_{WP}}\right)\left(\frac{\nabla_F}{\nabla}\right)^2 \end{aligned} \tag{5}$$

The *BM* and *KG* are changed as follows.

$$BM' = \frac{i_T}{\nabla'} = \frac{i_T}{\nabla + \nabla_F} \approx \frac{i_T}{\nabla}\left(1 - \frac{\nabla_F}{\nabla}\right) \quad (6)$$

$$\begin{aligned} KG' = \frac{KG\times\nabla + z_F\times\nabla_F}{\nabla+\nabla_F} = \frac{KG + z_F\times\frac{\nabla_F}{\nabla}}{1+\frac{\nabla_F}{\nabla}} \approx \left(KG + z_F \times \frac{\nabla_F}{\nabla}\right)\left(1 - \frac{\nabla_F}{\nabla}\right) \\ = KG - (KG - z_F)\times\frac{\nabla_F}{\nabla} - z_F\left(\frac{\nabla_F}{\nabla}\right)^2 \end{aligned} \quad (7)$$

As a result, the metacentric height (*GM*, playing as the important stability index) is changed as in the following equation within the first order of ∇_F/∇. The changed amount is due to the flooding

$$GM' = KB' + BM' - KG' = GM + \left\{d + \frac{1}{2}\frac{\nabla_F}{A_{WP}} - z_F - GM\right\}\frac{\nabla_F}{\nabla} \quad (8)$$

If the damaged compartment has no water in it before damage, the additional decrease in stability takes place. This is the decrease in *GM* due to the free surface effect.

$$\delta GM = \frac{i_F}{\nabla'} = \frac{1}{12}\frac{l_F s_F{}^3}{\nabla + \nabla_F} \quad (9)$$

Here, if the center of gravity of flooding water is below the draft, *GM*, except for the free surface effect, increases. Flooding water increases *GM* because the center of gravity is usually below the draft. The decrease in *GM* due to the free water surface effect is independent of the amount and location of flooding water. Changes in the center of buoyancy and center of gravity are related to the amount of flooding water and location. When the example ship is flooded, the change in *GM* according to the depth of the flooded water is shown in Figure 5.

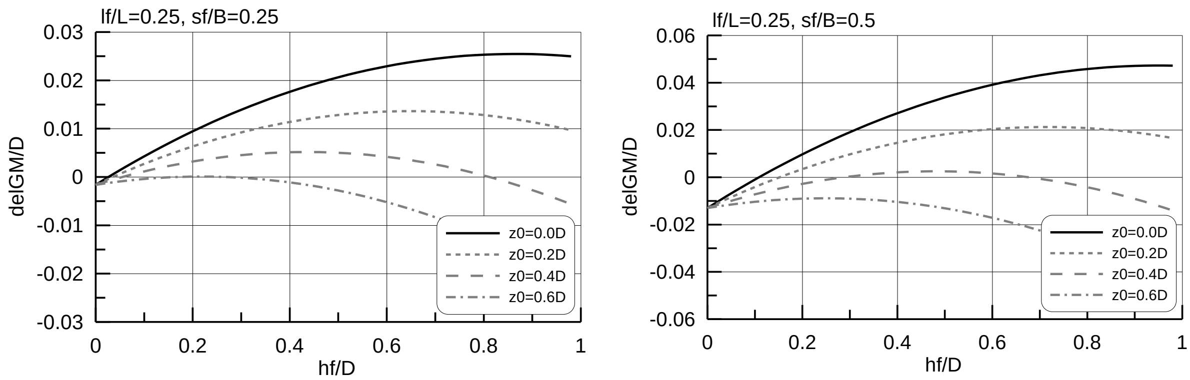

Figure 5. Changes in *GM*, according to the depth of the flooded water.

In Figure 5, the base height of the damaged compartment is denoted as z_0. When the height of the flooding water h_f, is zero, the *GM* change is negative due to the free surface effect. As the height of the flooding water increases, the *GM* change generally grows. However, the change of *GM* does not grow or decreases when the base height of the damaged compartment is high, above about 0.5D in this case. As shown above, the use of watertight compartments and lowering the inlet of the ventilation system can increase the stability of a damaged ship. However, it is important to check the change in *GM* to ensure that it remains positive in the event of any damage in order to prevent capsizing.

2. Buoyancy Support System (BSS) Implementation

2.1. A Small Car Ferry for BSS Implementation

Flooding accident cases with a risk of sinking were identified, and a buoyancy chamber installation plan was established. For the installation of the buoyancy chamber, the watertight area was considered first. It is hoped that the BSS can be installed on a ship the same size as the example ship in order to examine the flooding characteristics of watertight and non-watertight spaces, but it was difficult to find such a ship. For this reason, the installation of the BSS was aimed towards small car ferries powered by electric propulsion. These ferries operate on 800 kWh-class large-capacity batteries and carry a risk of short-circuit issues due to seawater inflow when sinking. BSS was first demonstrated via the application of a small electrically propelled car ferry launched in March 2022. Table 3 shows the small electric car ferry and its specifications. It is able to transport 120 passengers and 20 medium-sized vehicles simultaneously and uses two sets of 800 kWh mobile battery systems to transport passengers for a two-hour round trip in the West Sea of Korea.

Table 3. Specifications of target small car ferry subject to the BSS installation.

Image	Data	Value
	Length overall	Abt 60.00 m
	Length B.P. *	49.00 m
	Bredth (Max.)	13.00 m
	Bredth (Moulded.)	13.00 m
	Depth (Moulded)	3.150 m
	Draft (D.L.W.L. **)	1.630 m
	Draft (Scantling)	1.750 m
	Propulsion Motor	500 kW × 2 sets
	Speed (Service)	Abt. 10 knots
	Comlements	4 person
	Passenger	120 person
	Car (Midsize)	20 Unit

* Between Prependiculars. ** Designed Load Water Line.

2.2. Requirements for Residual Buoyancy

A small electric car ferry equipped with BSS has a vehicle deck from bow to stern. Figure 6 shows the layout of the watertight compartments of the target vessel.

Two trucks are located at the stern and used for transporting the mobile battery system for the power supply. Since this ferry mainly operates in an area of smooth waters, the freeboard is relatively low, and a bow ramp is installed for the boarding of both the vehicle and the passengers. Passengers can move to the cabin using the stairs or an elevator. The lower part of the vehicle deck is divided into more than 10 watertight spaces, and there is no separate watertight bulkhead separating the starboard and port areas based on the longitudinal centerline.

For the BSS design, a behavior simulation for a damaged ship was conducted, as shown in Table 4, assuming that up to two watertight spaces were damaged at the same time. In the case of a small car ferry, the division is simple and the hull shape is not complicated. Therefore, DELFTship [15], a commercial tool that is easy to access and use, was employed instead of the KRISO in-house tool for flood-scenario analysis. The use of commercial tools is intended to facilitate the creation of various types of BSS, even for small companies, using the results of this research for future reference. From the simulation results, cases of the target ship sinking occurred when void areas No. 1 and No. 2 were damaged at the same time. Based on this, the buoyancy chamber arrangement method applied to the BSS was reviewed.

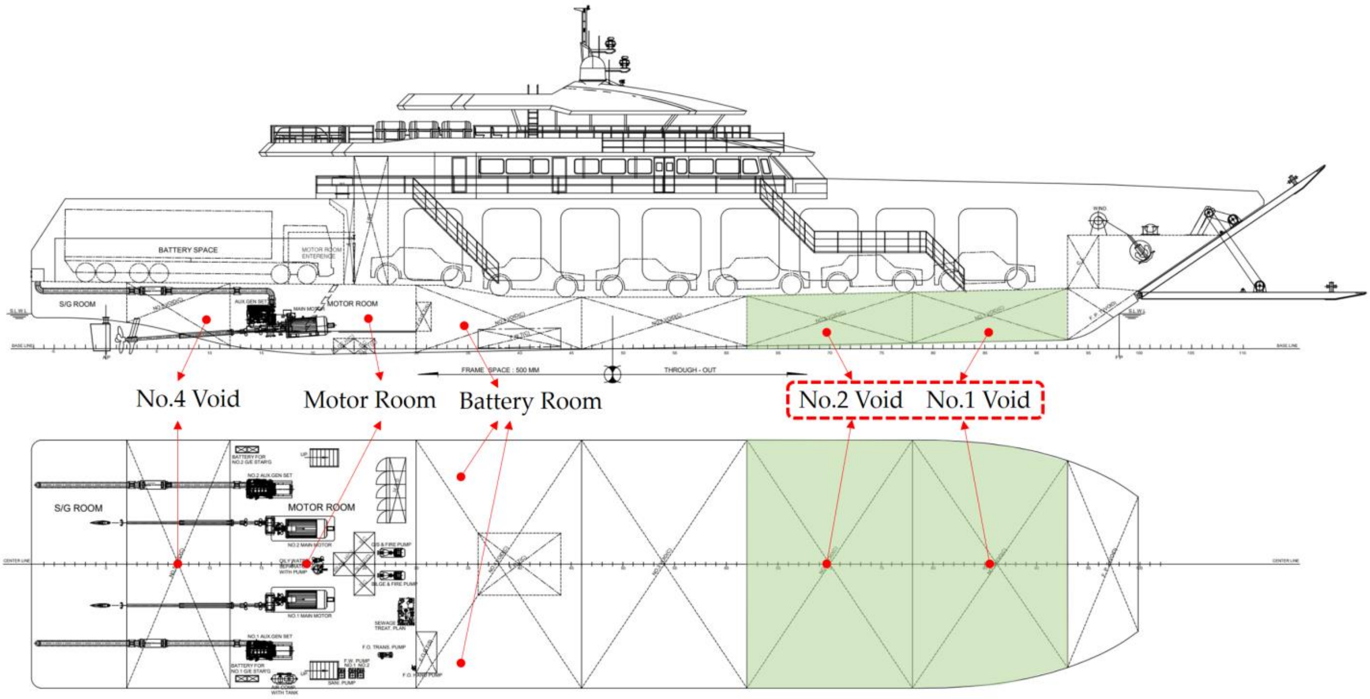

Figure 6. Compartment layout of target vessel.

Table 4. Examples of flooding accident cases where the target ship may sink.

	Damaged Zone	No. 1 Void	No. 1 Void	No. 1 Void	No. 1 Void	No. 1 Void	No. 1 No. 2 Void	No. 1 No. 2 Void	No. 1 No. 2 Void	No. 1 No. 2 Void	No. 1 No. 2 Void	No. 1 No. 2 Void	No. 1 No. 2 Void	No. 1 No. 2 Void
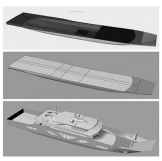	ITEM	LIGHT-SHIP	FULL LOAD. (Mid. Size Sedan)	FULL LOAD. (Mid. Size Sedan)	FULL LOAD. (Large Size Sedan)	FULL LOAD. (Large Size Sedan)	FULL LOAD. (Mid. Sedan + 25T Truck)	FULL LOAD. (Mid. Sedan + 25T Truck)	FULL LOAD. (5T Truck)	FULL LOAD. (5T Truck)	FULL LOAD. (25T Truck)	FULL LOAD. (25T Truck)	FULL LOAD. (Mid. Sedan + Mix. Truck)	FULL LOAD. (Mid. Sedan + Mix. Truck)
		-	Departure	Arrival	Departure	Arrival	Departure	Arrival	Departure	Arrival	Departure	Arrival	Departure	Arrival
	Condition No.	01	04	05	06	07	08	09	10	11	12	13	14	15
	GoM	O	O	O	O	O	Sink	Sink	O	O	Sink	Sink	Sink	Sink
	Marginline Surbmerging	O (Pt.22: −0.028)	O (Pt.22: −0.251)	O (Pt.22: −0.154)	O (Pt.22: −0.439)	O (Pt.22: −0.288)			O (Pt.22: −3.557)	O (Pt.22: −1.796)				

From the flooding simulation results for the accident scenarios in Table 4, it was determined that a small electric car ferry could sink if a hole with a diameter of 600 mm was made at the boundary between the No. 1 and No. 2 void areas. At this time, it was interpreted that it would take about 263 s for the small electric car ferry to sink. In order to prevent or delay sinking by installing buoyancy chambers in the No. 1 and 2 void areas, as shown in Figure 7, the deployment of the buoyancy chambers must be completed within 250 s, at which point the hull will start to sink rapidly.

In the simulation, sloshing due to flooding was not considered, and the characteristics of an actual flooding accident may be different from the simulation, such as during cargo loading. In addition to commercial tools such as DELFTship, it is necessary to apply analysis codes that consider gradual submersion and compressed air flows in the case of damage behavior analysis for large and complex ships. In this case, various guidelines and research results can be utilized [16–22].

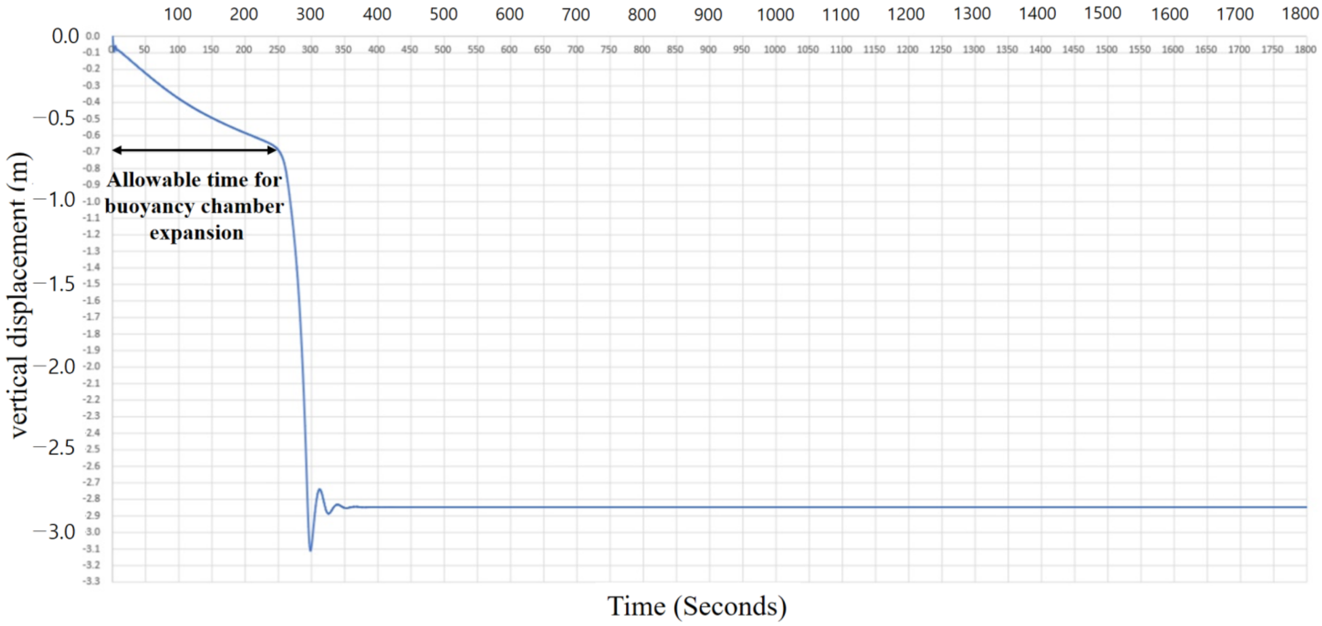

Figure 7. The results of the simulation of flooding due to damage to areas No. 1 and No. 2 void, sinking after 4.3 min (263 s).

In this case, it is believed that, in the event of a ship flooding accident, if the passengers can evacuate from the ship within 250 s, the target ship can be considered as secure even without the BSS. However, situations in which passengers must wear life jackets before escaping from the ship, or where the target ship lacks crew members to guide passengers, must be considered. In particular, if passengers who are gathered in the bow or stern muster station are waiting for another nearby ship or rescue team, the BSS can delay the sinking of the ship for a sufficient amount of time, thereby playing a meaningful role in securing passenger safety in a flooding emergency. Figure 8 shows evacuation simulation results based on Exodus [23]. Based on simulation results, it was confirmed that it would take from 89 to 142 s for passengers to evacuate depending on the direction: bow or stern. However, considering factors such as transportation-disabled individuals or panic in accident situations, it is expected that a much longer time may be required for an evacuation in real emergency situations. Therefore, even in situations where an evacuation is delayed, the BSS should be designed to deploy with sufficient time within 263 s, which is expected to be prior to the sudden sinking of the vessel.

According to SOLAS, whether a watertight area is divided into several parts has a great effect on damage stability [24]. Therefore, in a situation where it is difficult to further divide void areas No. 1 and No. 2, a plan to place a buoyancy chamber in these areas was considered.

The volume of void area No. 1 is 181.28 m^3. The volume of the buoyancy chamber must be at least 21.8 m^3 (12% of the volume of area No. 1) to secure residual buoyancy to prevent or postpone the sinking of the ship. In order to secure GoM where the margin line is not wetted, it is necessary to install a buoyancy chamber of 81.6 m^3 (45% of the volume of No. 1 area), but this is impossible considering the frame and web inside the hull. Therefore, a buoyancy chamber with a volume of abt. 49.8 m^3 (27% of the volume of the No. 1 area) was installed to prevent sinking in the simulation. Figure 9 shows the results of reviewing the installation space of the No. 1 area, and the design of the cylindrical buoyancy chamber, which is installed in this area.

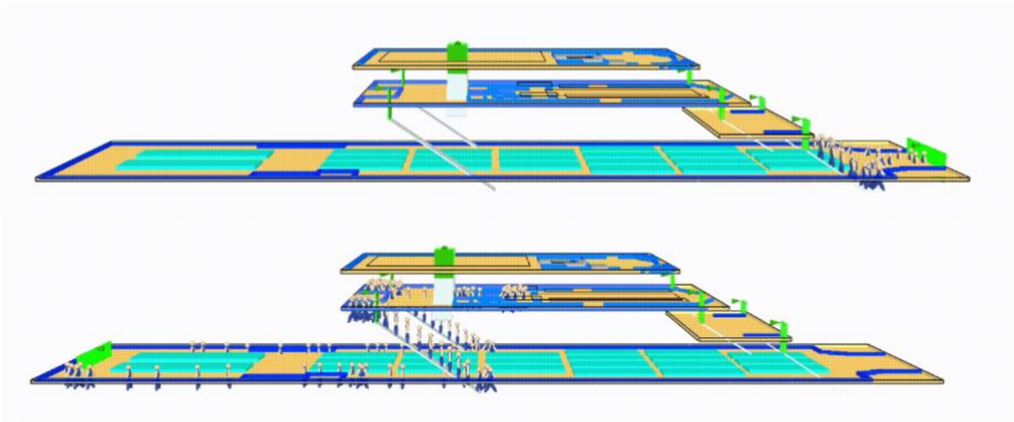

Figure 8. Examples of evacuation simulation. Evacuation took 89 s in the bow direction (**above**) and took 142 s in the stern direction (**below**).

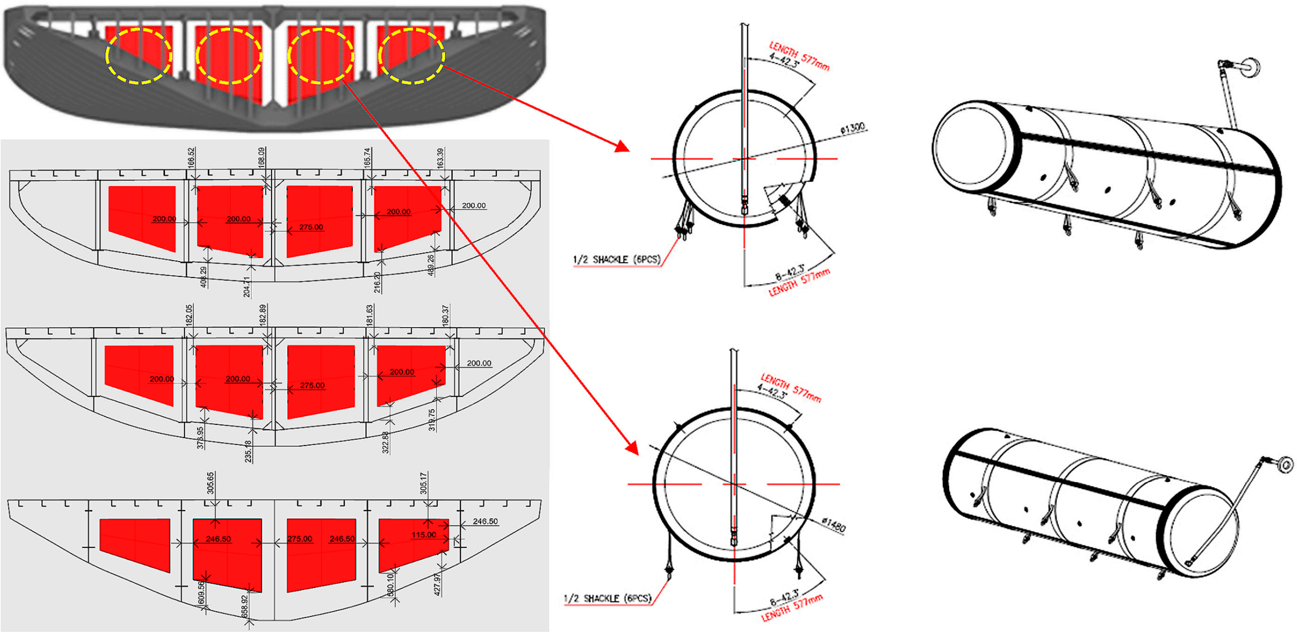

Figure 9. Example of the BSS installation space analysis and buoyancy chamber design.

The red rectangle on the cross-section of Void Area No. 1 shows the space where the buoyancy chamber can be installed. The circular dotted line indicates the installation position of the cylindrical buoyancy chamber. The adoption of a cylindrical buoyancy chamber prevents damage due to the concentration of pressure on a specific section in the process of being folded and expanded for a long time. When a cylindrical buoyancy chamber is applied, the volume of the buoyancy chamber is approximately 30 m^3 (16.6% of the volume of the No. 1 void area).

The volume of the adopted buoyancy chamber can prevent the sinking of the small electric car ferry in the accident scenario but may be insufficient considering that the buoyancy chamber can be installed up to 49.8 m^3. Therefore, as shown in Table 5, simulations were also performed to assess sinking prevention via the installation of the buoyancy chamber. The results of the simulation confirm that it would be difficult to secure an evacuation space in the bow with a 30 m^3 buoyancy chamber that would not be submerged. However, an evacuation space could still delay sinking, and it was confirmed that access to the stern of the rescue vessel and the escape of passengers would be possible.

Table 5. Simulation results according to the volume of the buoyancy chamber.

Buoyancy Chamber: NA			**Buoyancy Chamber: 22 m^3**			**Buoyancy Chamber: 30 m^3**			**Buoyancy Chamber: 49.8 m^3**		
Light-ship weight		580.0	Light-ship weight		580.0	Light-ship weight		580.0	Light-ship weight		580.0
Displacement		780.2	Displacement		943.7	Displacement		780.2	Displacement		780.2
Draft	(dF) (m)	-	Draft	(dF) (m)	5.902	Draft	(dF) (m)	4.414	Draft	(dF) (m)	3.446
	(dM) (m)	−1847		(dM) (m)	3.259		(dM) (m)	2.760		(dM) (m)	2.465
	(dA) (m)	-		(dA) (m)	0.617		(dA) (m)	1.106		(dA) (m)	1.484
Trim(AFT:-) (m)		-	Trim(AFT:-) (m)		5.285	Trim(AFT:-) (m)		3.307	Trim(AFT:-) (m)		1.962
L.C.G		22.571	L.C.G		25.995	L.C.G		22.571	L.C.G		22.571
L.C.F		-	L.C.F		12.136	L.C.F		13.990	L.C.F		22.695
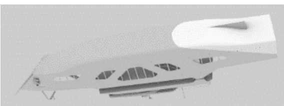			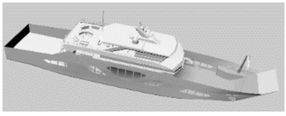			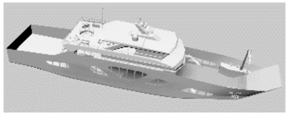			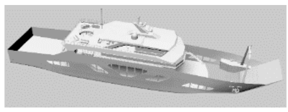		
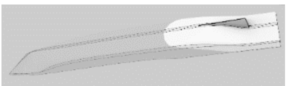			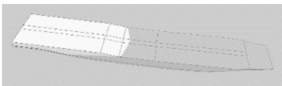			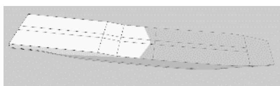			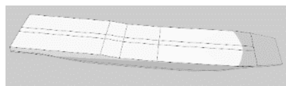		
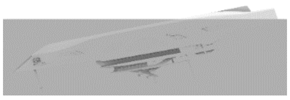			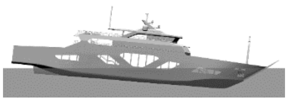			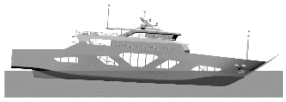			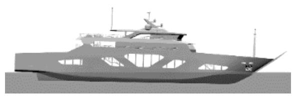		
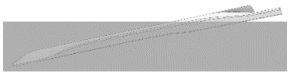			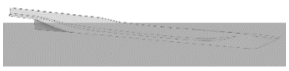			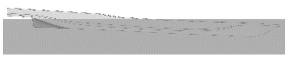			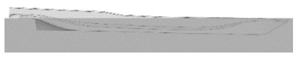		
			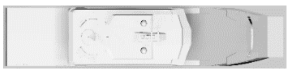			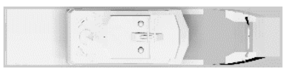			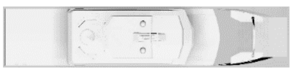		

In order to prevent damage to the buoyancy chamber during expansion due to collisions of the damaged and sharpened hull plates, buoyancy chambers were not installed either at the port or starboard ends of the No. 1 and No. 2 void areas. In addition, the gas inlet nozzle and the buoyancy chamber are separately arranged so that even if one buoyancy chamber is damaged, the other buoyancy chambers are not affected.

2.3. BSS Design for Target Vessel Installation

Assuming the use of a fixed fire main to inflate the buoyancy chamber, it is necessary to consider the injection temperature of carbon dioxide. Although it is not mentioned in ISO 23121-1, the problem of damage to the buoyancy chamber due to low temperatures must be considered because carbon dioxide will be injected into the buoyancy chamber at −68 °C. First, considering the low carbon dioxide temperature, a method of making the material of the buoyancy chamber thicker can be considered. However, there is a limit to increasing the thickness due to the characteristics of the buoyancy chamber, which must be folded and stored normally and not be too heavy.

Therefore, a method of applying a heat exchanger to lower the temperature of carbon dioxide injected into the buoyancy chamber was reviewed. Through an experimental method, the carbon dioxide injection temperature, which does not damage the buoyancy chamber, was set to −10 °C. In order to lower the injection temperature of carbon dioxide without a heat exchanger, a pipe with a diameter of 1.5 inches is required more than 7000 m when the wind speed is 0 m/s, 280 m when the wind speed is 5 m, and 190 m when the wind speed is 10 m. Figure 10 shows an example of a pipeline diagram for BSS configuration and the effect of temperature change due to the convective effect without a heat exchanger.

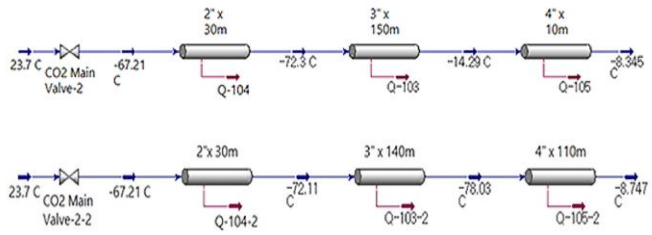

Figure 10. Example of temperature drop design according to the length of the carbon dioxide transfer line; at wind speed: 10 m/s (**above**), 5 m/s (**below**).

When applying the heat exchanger, the method of using seawater by utilizing the characteristics of the ship was reviewed. When the heat exchanger was configured, as shown in Figure 11, by drawing in seawater from the outside of the ship to increase the temperature of the carbon dioxide injection pipe, the carbon dioxide injection temperature could be raised from −68 °C to −7.3 °C.

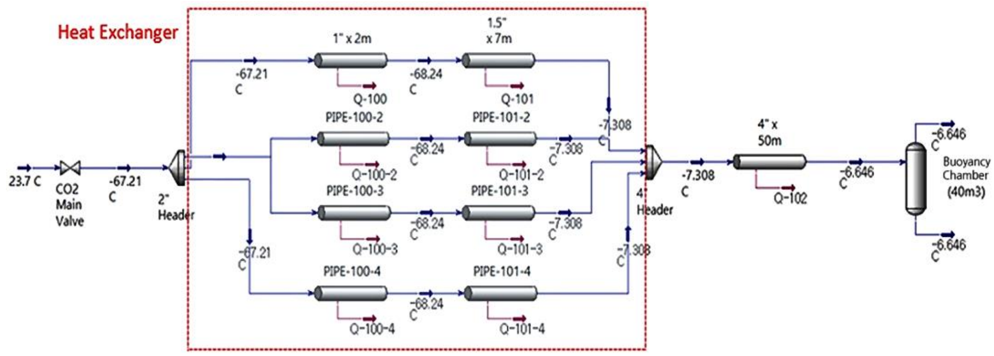

Figure 11. Example of pipe line diagram for when a heat exchanger is applied.

A total of four buoyancy chambers were installed on the small electric car ferry, and the volume was 30 m^3. The number of carbon dioxide cylinders and nozzle specifications were set so that the buoyancy chamber was fully deployed within 250 s from the simulation results in Figure 7. For ships, the carbon dioxide in the cylinder is compressed to 58 Bar, and the density of carbon dioxide at atmospheric pressure and at room temperature (25 °C) is 1.78 kg/m^3. As the density of seawater is 1024 kg/m^3, 1.75 kg of carbon dioxide will generate 1.024 tons of buoyancy. Since carbon dioxide cylinders for ships weigh 45 kg each and have a 90% filling rate, it is possible to inject 25.28 m^3 of carbon dioxide and generate 25.87 tons of buoyancy per cylinder. Table 6 shows design specifications for considered buoyancy chamber to install.

Table 6. Buoyancy chamber design specifications.

Data	Value	Note
Buoyancy chamber volume	30.08 m^3	8.91 m^3 2ea, 6.13 m^3 2ea
Permissible inner pressure	1.5 bar g (2.513 bar a)	Bar g: gauge, a: absolute
Design temperature for CO_2 injection	−10 °C	-
Inflation time	Within 250 s	-

The density of carbon dioxide inside the BSS is 5.2167 kg/m^3 [25] when carbon dioxide is charged at 2.513 bar at −10 °C, and 156.5 kg of carbon dioxide is required to fill a 30 m^3 buoyancy chamber. Therefore, four carbon dioxide cylinders with a capacity of 45 kg must be applied to the BSS configuration. A check valve must be installed in the buoyancy chamber to discharge carbon dioxide that is charged above the allowable pressure. Since the target ship operates in a calm sea, the water pressure is not expected to be high during BSS expansion. Carbon dioxide is injected into the buoyancy chamber at a pressure of 58 bar. Therefore, the situation where the BSS needs to be inflated in a completely submerged area is not considered. Table 7 shows the pressure and temperature simulation result for the buoyancy chamber inflation.

Table 7. Pressure and temperature simulation result for the buoyancy chamber inflation.

Data	Pressure (Bar)	Temperature (°C)	Flow Rate (kg/s)
Carbon dioxide cylinder	58.0	21.0	0.3750
Inlet to buoyancy chamber	1.0	−68.0 (N/A) −10.0 (with heat exchanger)	0.0136

Figure 12 shows the BSS design result for the installation of a small electric car ferry on the basis of a fixed fire-fighting system. The buoyancy chambers are installed in four parts in the No. 1 void area and inflated using four 45 kg-capacity carbon dioxide cylinders. A heat exchanger using seawater is installed to prevent the buoyancy chamber from being damaged by low temperatures when carbon dioxide is injected. The BSS can be automatically operated with a flooding detection system, but a controller that can operate the BSS after checking the accident situation was installed on the bridge due to the nature of a small electric car ferry that always has a crew on the bridge.

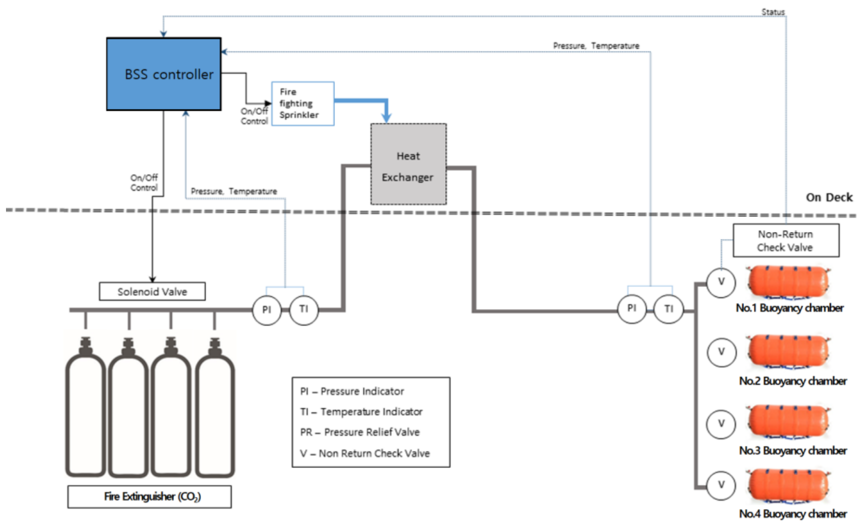

Figure 12. P and I diagram of the BSS.

2.4. Prototype and Verification, Ship Installation

According to the design results, a BSS for a small electric car ferry was developed. The buoyancy chamber of the No. 1 void area was placed on the floor, and the carbon dioxide injection pipe was applied with a flexible hose to withstand an impact in case of damage, such as a collision. There is no approval procedure for a BSS, so this system was mainly composed of class-certified products. After installing a small electric car ferry, it received a third-party verification from the Korean Register of Shipping. Figure 13 shows the process of installing a BSS on a small electric car ferry and process for the third-party verification of the Korea Register of Shipping.

Figure 13. Prototype test (**above**) and target ship installation (**below**). Third-party verification certificate (**below right**) of the BSS.

As a result of third-party verification, the BSS installed in the small electric car ferry was evaluated to have secured the required performance and was issued a certificate in October 2022. However, the carbon dioxide injection system of the BSS was installed separately from the fixed fire main. This is because the area with the highest fire risk is located far from the area where the buoyancy chamber is installed, and there is no legal basis for using a fixed fire main for purposes other than fire extinguishing.

3. Application Expansion Plan

The BSS can contribute to minimizing loss in the event of an accident when installed and operated in areas with a high risk of sinking in case of flooding, such as the machinery room and car deck. To this end, it is necessary to secure a case in which a number of cylinder-shaped buoyancy chambers are arranged, or a three-dimensional buoyancy chamber is configured and installed in a complex area, such as a machinery room. Figure 14 shows an example of acquiring 3D cloud point data and arranging a buoyancy chamber to apply BSS to the machinery room of a large ship.

Vol. Ratio	Vol. of Buoyancy Chamber
70%	338.37 m^2/237.38 m^2
50%	338.37 m^2/170.21 m^2
30%	338.37 m^2/100.34 m^2

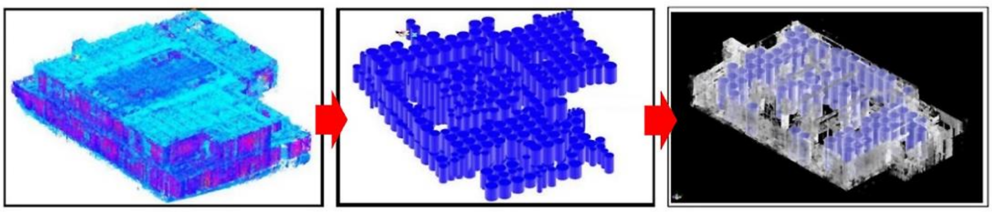

Figure 14. Case study result of 3D point cloud data basis buoyancy chamber arrangement in the machinery room.

In order to apply BSS to the machinery room of a large ship, research is underway regarding how to apply BSS to K-GTB, an eco-friendly alternative fuel and electric propulsion system demonstration ship. The K-GTB is under construction after the steel cutting ceremony in September 2022 and is scheduled to operate from 2024. The K-GTB shape and specifications are shown in Figure 15.

Figure 15. BSS to be equipped; 2600 GT class K-GTB appearance and specifications.

Figure 16 shows the general arrangement of the K-GTB. The BSS is designed with consideration of the installation of the machinery room and the alternative fuel demonstration area near the midship, where the MW class battery, fuel cell, and carbon-free fuel mixed combustion engine systems are installed.

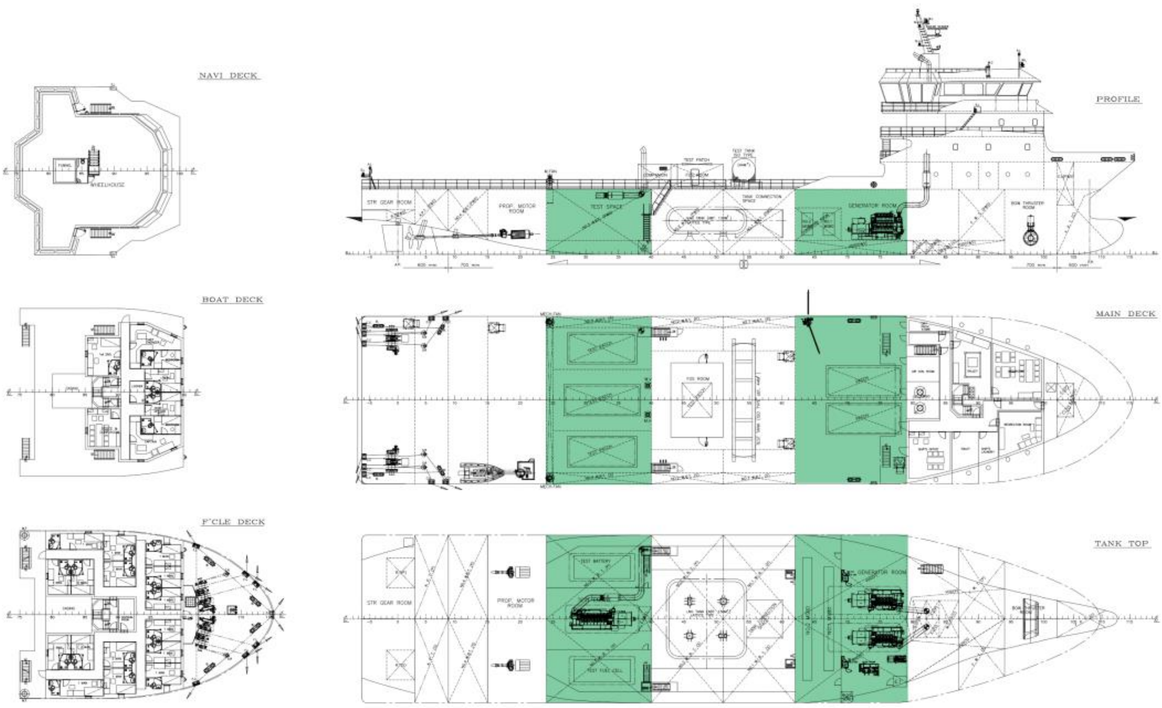

Figure 16. Conceptual design and location of BSS installation, as verified by the general arrangement of K-GTB.

BSS for K-GTB implementation is under development, as shown in Figure 17. A three-dimensional buoyancy chamber prototype was made, and the operability of its heat exchanger is being tested on land. A plan to reduce the size of the heat exchanger and divide the buoyancy chamber into several inner airtight areas to minimize the loss of residual buoyancy when the buoyancy chamber is damaged is also being devised.

Figure 17. BSS prototype test for installation in a K-GTB machinery room.

4. Conclusions

This study focuses on the BSS, which was first introduced in 2018 and designed for use on actual ships. The study reviewed existing technologies for securing residual buoyancy and proposed a new design alternative called BSS, which was found to be both technically and economically feasible. Simulation results using the KRISO in-house tool were also presented. In 2022, the proceedings presented at PRADS introduced the development process of applying the BSS to a small electric propulsion car ferry. The study involved manufacturing and testing prototypes of BSS and evaluating their implementation in a real ship. The study proposed that BSS, which considers the flooding characteristics of watertight and non-watertight spaces and uses a fixed fire main, can minimize damage in case of an accident, while also minimizing cost burden. Furthermore, the study describes the concept of applying BSS to large ships, particularly in complex areas such as machinery rooms. BSS operation in such areas can be advantageous in terms of minimizing accident damage and quick damage recovery, which is important for SRtP (Safe Return to Port). The study suggests that BSS can contribute to improving maritime safety as an affordable alternative that can minimize the loss of life, environment, and property, even in the event of serious damage or flooding that exceeds design criteria.

Author Contributions: Conceptualization, G.J.L. and H.J.K.; methodology, H.J.K. and K.K.L.; software, K.K.L.; validation, H.J.K. and J.-P.H.; writing—original draft preparation, H.J.K.; writing—review and editing, H.J.K. All authors have read and agreed to the published version of the manuscript.

Funding: This study was supported by a grant from the National R&D Project "Development of 1 MW class Marine Test-bed for Adoptability Demonstration of Alternative Fuels" funded by the Ministry of Oceans and Fisheries of Korea [1525012293/PMS5560].

Institutional Review Board Statement: Not applicable.

Informed Consent Statement: Not applicable.

Data Availability Statement: Not applicable.

Acknowledgments: The authors would like to express their sincere gratitude to the support from the Ministry of Oceans and Fisheries, Republic of Korea. The authors would also like to thank LEEYONGSND Corporation for their contribution to this study, as well as their support in writing this paper.

Conflicts of Interest: The authors declare no conflict of interest.

References

1. Kang, H.J.; Kim, I.; Choi, J.; Lee, G.J.; Park, B.J. A concept study for the buoyancy support system based on the fixed fire-fighting system for damaged ships. *Ocean. Eng.* **2018**, *155*, 361–370. [CrossRef]
2. ISO. ISO 23121-1:2019. Available online: https://www.iso.org/standard/74624.html (accessed on 30 December 2022).
3. ISO. ISO 23121-2:2019. Available online: https://www.iso.org/standard/74625.html (accessed on 30 December 2022).
4. Kang, H.J.; Lee, K.K.; Lee, D.K.; Kim, Y.S. *Real Ship Implementation of Buoyancy Support System for Damaged Ships*; PRADS: Dubrovnik, Croatia, 2022.
5. Trimulyono, A.; Fuadi, M.A.; Zakki, A.F.; Mursid, O.; Iqbal, M. Design of anti-capsize ship for patrol vessel with the self-righting moment. *J. Mar. Sci. Eng.* **2023**, *11*, 133. [CrossRef]
6. Vassalos, D.; Paterson, D.; Mauro, F.; Atzampos, G.; Assinder, P.; Janicek, A. High-expansion foam: A risk control option to increase passenger ship safety during flooding. *Appl. Sci.* **2022**, *12*, 4949. [CrossRef]
7. Valanto, P. Active Flooding Mitigation for Stability Enhancement in a Damaged RoPax Ship. *J. Mar. Sci. Eng.* **2022**, *10*, 797. [CrossRef]
8. Pan, D.; Sun, Y.; Zhou, Z.; Zhao, K.; Chen, Y. Calculation on Refloating a damaged ship with salvage pontoon. *IOP Conf. Ser. Mater. Sci. Eng.* **2020**, *772*, 012078. [CrossRef]
9. Bačkalov, I.; Bulian, G.; Rosén, A.; Shigunov, V.; Themelis, N. Improvement of ship stability and safety in intact condition through operational measures: Challenges and opportunities. *Ocean Eng.* **2016**, *120*, 353–361. [CrossRef]
10. Boulougouris, E.; Cichowicz, J.; Jasionowski, A.; Konovessis, D. Improvement of ship stability and safety in damaged condition through operational measures: Challenges and opportunities. *Ocean Eng.* **2016**, *122*, 311–316. [CrossRef]
11. Vassalos, D.; Boulougouris, E.; Paterson, D. An alternative system for damage stability enhancement. In Proceedings of the 15th International Ship Stability Workshop, Stockholm, Sweden, 13–15 June 2016; pp. 1–6.
12. Smith, C.; Volonakis, S.; Chatzidouros, E.; Zilakos, I. Definition of a Buoyancy Rescue Concepts for Three Scenarios. SUSY Consortium. 2011. Available online: https://trimis.ec.europa.eu/sites/default/files/project/documents/20120405_230626_86293_SUSY%20D-2-4%20Definition%20of%20buoyancy%20rescue%20concepts_public.pdf (accessed on 30 December 2022).
13. Lee, G.J. Dynamic orifice flow model and compartment models for flooding simulation of a damaged ship. *Ocean Eng.* **2015**, *109*, 635–653. [CrossRef]
14. Process Engineer's Tool, Valves and Fittings Pressure Drop Coefficient K. Available online: https://powderprocess.net/Tools_html/Piping/Pressure_Drop_Key_Piping_Elements_K_Coefficient.html (accessed on 30 December 2022).
15. Delftship Maritime Software. DELFTship: Visual Hull Modelling and Stability Analysis. Available online: https://www.delftship.net/ (accessed on 30 December 2022).
16. Choi, J.; Lee, D.; Lee, G.; Kang, H.J.; Kim, K. Development of a Safety Assessment System for a Damaged Ship Based on NAPA. *J. Ships Ocean Eng.* **2010**, *49*, 89–95.
17. Ruponen, P.; Larmela, M.; Pennanen, P. Flooding prediction onboard a damaged ship. In Proceedings of the 11th International Conference on the Stability of Ships and Ocean Vehicles, Athens, Greece, 23–28 September 2012.
18. Dankowski, H. A Fast and Explicit Method for Simulating Flooding and Sinkage Scenarios of Ships. Ph.D. Thesis, Technischen Universität Hamburg, Harburg, Germany, 2013. Available online: http://tubdok.tub.tuhh.de/handle/11420/1127 (accessed on 30 December 2022).
19. Pekka, R. Adaptive time step in simulation of progressive flooding. *Ocean Eng.* **2014**, *78*, 35–44.
20. Luca, B.; Mauro, F. A new calculation technique for onboard progressive flooding simulation. *Ship Technol. Res.* **2019**, *66*, 150–162.
21. Lee, G.J. Self-similarity in the equation of motion of a ship. *Int. J. Nav. Archit. Ocean Eng.* **2014**, *6*, 333–346. [CrossRef]
22. Lee, G.J. Moment of inertia of liquid in a tank. *Int. J. Nav. Archit. Ocean Eng.* **2014**, *6*, 132–150. [CrossRef]
23. Fire Safety Engineering Group, University of Greenwich. Exodus Model Briefly Explained. Available online: https://fseg.gre.ac.uk/exodus/work.html (accessed on 30 December 2022).
24. IMO. SOLAS. Available online: https://www.imo.org/en/KnowledgeCentre/ConferencesMeetings/Pages/SOLAS.aspx (accessed on 30 December 2022).
25. Peace Software. Available online: http://www.peacesoftware.de/einigewerte/co2_e.html (accessed on 30 December 2022).